15th International Symposium on Practical Design of Ships and Other Floating Structures PRADS 2022

Dubrovnik, Croatia, October 9th – 13th 2022

Hydrodynamic Studies on a Zero Emission Battery-Driven Fast-Ferry

Yan Xing-Kaeding[1,*], Apostolos Papanikolaou[2], Aphrodite Kanellopoulou[2], George Dafermos[2] and George Zaraphonitis[2]

[1] Hamburgische Schiffbau-Versuchsanstalt GmbH/HSVA, Hamburg, GERMANY

[2] National Technical University of Athens, GREECE

Abstract. This paper presents extensive experimental and numerical CFD studies focusing on the optimisation of the hull form and propulsion of a novel, battery-driven, fast shortsea catamaran. Numerical results of the achieved speed-power performance and of the very high propulsive efficiency of close to 80% were verified by model experiments at the Hamburgische Schiffbau Versuchsanstalt (HSVA), proving the feasibility of the concept. Additional numerical investigations have been conducted recently on the seakeeping and manoeuvrability of the vessel. The seakeeping characteristics of the vessel have been comparatively studied by the potential flow code NEWDRIFT of NTUA and the RANS code FreSCO+ of HSVA, showing a reasonably good agreement. The turning manoeuvring of the catamaran has been simulated in time domain by the RANS method, with the catamaran fitted with up to four propulsors (two propellers plus two bow thrusters) operating simultaneously. The manoeuvrability of the vessel proved satisfactory, while the simulated physical phenomenon showed a very complex free surface deformation and flow around the vessel. The subject vessel is designed in the framework of the Horizon 2020 European Research project "TrAM – Transport: Advanced and Modular" (2018-2022). Presently, a prototype of the vessel named "Medstraum" is on the delivery stage and it will start operations on a multi-stop commuter route in the Stavanger area, Norway, before the end of 2022.

Keywords: *battery-driven ship, all electric, fast-ferry, zero emissions, catamaran design, parametric model, hydrodynamic optimisation, high propulsive efficiency, CFD validation, RAOs in seaway, seakeeping, manoeuvring.*

1. Introduction

The work presented in this paper is conducted in the frame of the Horizon 2020 European Research project "TrAM – Transport: Advanced and Modular", which is a joint effort of 13 stakeholders of the European maritime industry [1]. The aim of this project is to develop zero emission fast going passenger vessels through advanced modular production, with the main focus on electrically powered vessels operating in coastal areas and inland waterways. The project is innovative for the introduced zero emission technology, the design and manufacturing methods, while it should prove that electric-powered vessels can be fast and competitive in terms of offered services, building and the life-cycle cost, and of course especially in terms of the environmental footprint.

In the frame of this project, intensive research has been carried out on the different aspects of hydrodynamic studies, such as the hydrodynamic optimisation of a battery-driven catamaran's hull form and investigations on the seakeeping and manoeuvring behaviours. The aim of the hydrodynamic optimisation was to minimise the hull resistance, the associated propulsion power requirements and energy consumption. This was enabled by the multi-stage optimisation of the catamaran's hull form and the local optimisation of its transom stern, including its interaction with all the propulsive devices, namely the fitted propellers, rudders, propeller shafts and brackets. It should be noted that present energy density of the battery with respect to both energy per volume and per weight is very much lower than that of conventional fossil fuel, which leads to the conclusion that the battery-driven waterborne concept will be (in the foreseeable future) limited to the lower and medium speed range due to inherent limitations on the installed battery capacity/weight [2]. In that respect, hydrodynamic (as well as minimum structural and outfitting weight) optimisation is for battery-driven fast vessels imperative for the success of the concept.

A demonstrator of the presently studied catamaran concept named Medstraum was built at Fjellstrand shipyard (see Fig. 1) and will start operations in a multi-stop commuter route in the Stavanger area, Norway, before the end of the project in 2022 (https://tramproject.eu/).

* Correspondence to: xing-kaeding@hsva.de

Figure 1. Medstraum's main structure (Fjellstrand shipyard) (source: https://www.fjellstrand.no/)

2. Numerical Methods

A variety of numerical methods have been applied in the hydrodynamic analysis and optimisation study of the subject catamaran, starting from the use of the CAD and optimisation software platform CAESES® with the development of surrogate models for the ship's resistance based on calculations for a large number of design variants using HSVA's panel code v-SHALLO and the RANS based CFD code FreSCo+ and the multi-objective global and local optimisation by use of genetic algorithms. The 3D panel code NEWDRIFT from NTUA has been used for the calculation of the seakeeping responses of ships and floating structures, excited by incident regular waves. The RANS code FreSCo+ has been again employed for the confirmation of the vessel responses in seaway predicted by NEWDRIFT and detailed study on the turning-manoeuvres of the vessel.

2.1. Potential Flow Method

2.1.1. HSVA's panel code v-SHALLO

HSVA's panel code v-SHALLO is a fully non-linear, free surface potential CFD method computing the inviscid flow around a ship hull moving on the free water surface. The code is based on a superposition of a given free stream velocity with the flow induced by a number of 3D Rankine point sources on the ship's hull and the free surface. v-SHALLO is treating the nonlinear free surface boundary condition iteratively by a collocation method and uses a patch method for dealing with the body boundary condition and pressure integration [3, 4]. The hull and the free surface are discretised by means of triangular and/or rectangular panels and the individual source strengths are determined by solving a linear equation system resulting from the discretisation of a Fredholm integral equation.

The applied panel mesh for the demihull of the catamaran is shown in Figure 2 as an example. Trim and sinkage are estimated based on the vertical forces and the body grid is moved accordingly. The wave elevation at the collocation points is computed from Bernoulli's equation. A typical wave pattern computed for the Stavanger demonstrator at a speed of 23 kn is shown in Figure 3.

Figure 2. Discretised demihull of the Stavanger demonstrator

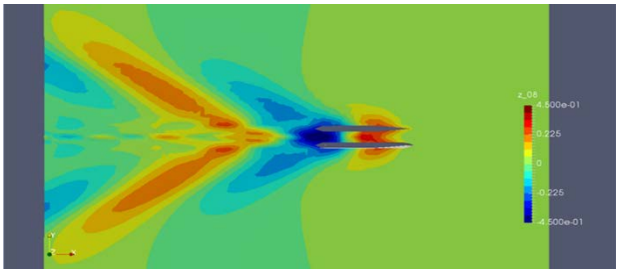

Figure 3. Wave Pattern of the Stavanger demonstrator at 23 kts

2.1.2. NTUA's code NEWDRIFT

NEWDRIFT is a potential 3D panel code for the calculation of the seakeeping responses of ships and floating structures, excited by incident regular waves.

NEWDRIFT is based on the Green Function's method, using a distribution of 3D pulsating sources for the description of the velocity potential, which is a special sub-category of the general Boundary Elements Methods (BEM). The basic distinguishing characteristic of these methods from other BEM methods, is that the distribution of sources is limited to the (mean) wetted surface of the floating body, hence the free surface does not need to be discretized. This is achieved as a suitable Green function, satisfying all boundary conditions, save for the kinematic boundary condition on the wetted surface, is employed. The total velocity potential is expressed as the linear superposition of the incident, diffraction and radiation potentials. Once the diffraction and radiation potentials are calculated, the exciting forces and hydrodynamic coefficients (added masses and damping) are evaluated, leading to the calculation of the body motions, velocities and accelerations in 6 DOF. For the numerical implementation of the code, the discretization of the demihull is likewise v-SHALLO conducted by use of a set of triangular and/or quadrilateral elements, see Fig. 4 for an example of the applied panel mesh. A more detailed description of the theoretical background and validation of the code can be found in [5, 6], while noting that code is free of the so-called "irregular frequencies" problem thanks to the introduced remedy by Dafermos et. al. [7].

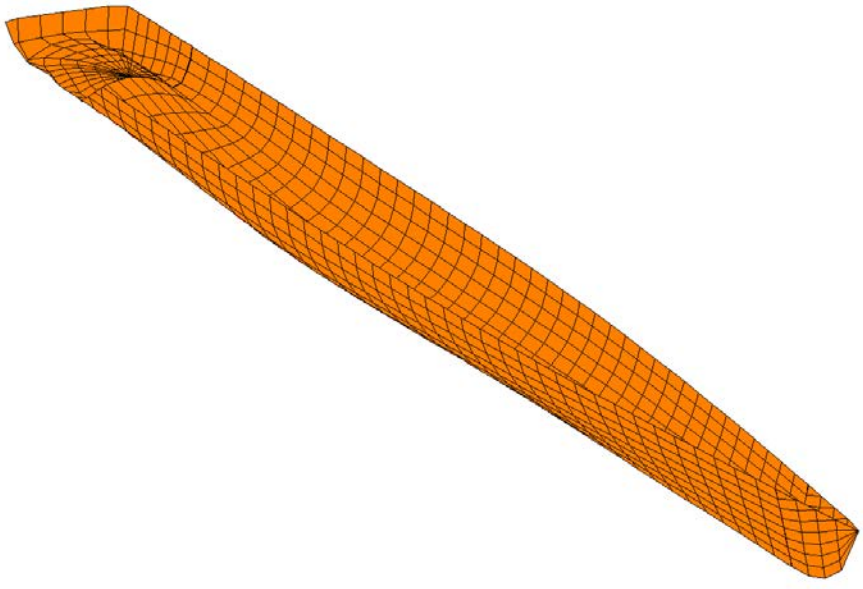

Figure 4. Discretisation of demihull by 1330 panels (code NEWDRIFT)

2.2. RANSE Method

The HSVA in-house code FreSCo+ [8] is a finite volume fluid flow solver developed in cooperation with the Institute of Fluid Dynamics and Ship Theory (FDS) of the Hamburg University of Technology (TUHH) and the

Hamburg Ship Model Basin (HSVA). Emphasis is thereby placed on an important element of maritime problems, namely the prediction of the free surface flow around ships, which is expressed in the name FreSCo, standing for Free Surface Computation.

The computational method in 'FreSCo+' is based on a finite-volume method and allows both structured-grid and unstructured-grid discretisation. FreSCo+'s mathematical model is essentially the Reynolds-averaged Navier-Stokes (RANS) equations, supplemented with a series of turbulence models based on the eddy viscosity concept and a treatment of multi-phase flows using the volume-of-fluid approach. The FreSCo+ code solves the incompressible, unsteady Navier-Stokes-equations (RANSE). The transport equations are discretized with the cell-centered finite volume method. Using a face-based approach, the method is applied to fully unstructured grids using arbitrary polyhedral cells or hanging nodes.

The governing equations are solved in a segregated manner, utilizing a volume-specific pressure correction scheme to satisfy the continuity equation. To avoid an odd-even decoupling of pressure and velocity, a third-order pressure smoothing is employed along a route outlined by [9]. The solution is iterated to convergence using a SIMPLE-type pressure-correction scheme. The fully-implicit algorithm is second order accurate in space and time. The approximation of the integrals is based on the mid-point rule. Diffusion terms are approximated using second-order central differences, whereas advective fluxes are approximated based on blends between high-order upwind-biased schemes (e.g. QUICK), first order upwind and second order central differences schemes. The latter are applied in scalar form by means of a deferred-correction approach.

The method is applied to fully unstructured grids using arbitrary polyhedral cells or hanging nodes. Also, features such as sliding interface or overlapping grid techniques have been implemented into the code [10]. Various turbulence-closure models are available for application, such as k-ε (Standard, RNG, Chen), k-ω (Standard, BSL, SST), Menter's One Equation model and the Spalart-Allmaras turbulence model. In this paper, the k-ω SST model has been mainly used.

The RANS code 'FreSCo+' has been coupled with the HSVA in-house panel code "QCM" to numerically simulate the self-propulsion test [11]. The method implemented in the "QCM" code is a vortex lattice method (VLM). The blades of the propeller are reduced to lifting surfaces which account for camber and angle of attack. The lifting surfaces are built up by section mean lines. The thickness effect is accounted for by prescribed source densities on the lifting surfaces. The present local hullform optimisation studies aiming at very high propulsive efficiency have been performed using the RANS-QCM coupling approach, where the code FreSCo+ is coupled with QCM for propeller analysis in an iterative fashion as sketched in Figure 5.

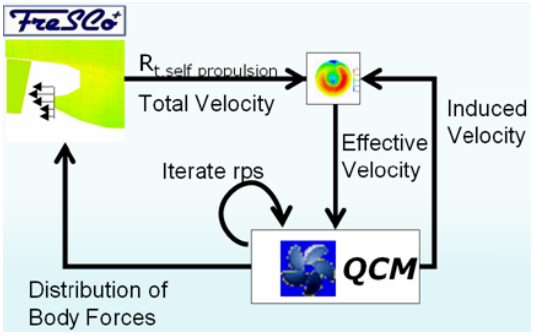

Figure 5. Numerical Self-Propulsion Test Scheme by FreSCo+ and QCM

At the start of the simulation, a nominal wake distribution is extracted from the converged RANS solution without the propeller effect. This velocity distribution and an estimated turning rate are used as an input for the QCM code to compute the forces on the propeller blades (thrust and torque). The turning rate is adjusted until the propeller thrust required to overcome the ship resistance (in propulsion mode) is obtained. The hydrodynamic forces of the propeller are converted in the form of 3D body forces (source terms) assigned to cells which are representing the propeller disk.

The resulting distribution of the body forces is used as an input to a next RANS calculation loop. The RANS computation is continued in the next iteration cycle and a new total velocity field is created. The propeller induced velocities of the previous cycle, which are an output of the QCM code, are subtracted from the total velocity field. The resulting effective wake distribution is used as input in the subsequent QCM calculation. The iteration is repeated until the equilibrium between the resistance of the ship under self-propulsion condition and the propeller thrust is reached. More details of this method and its application can be found in [12].

3. Hydrodynamic Optimisation

A brief description on the conducted hydrodynamic optimisation work will be given in this section; emphasis will be put on the process of development from the practical design point of view. More details on the results have been published and can be found in [13, 14, 15].

3.1. Characteristics of the Stavanger Demonstrator

The external dimensions of the vessel facilitating the required passengers transport capacity were set equal to 31.0m length overall by 9.0m beam overall. The vessel should be able to carry up to 147 passengers with a maximum operating speed of about 23-25 kn, depending on the loading condition and installed power of the propulsion e-motors. The overall length of each demihull was set equal to 30.6m. Because of uncertainties in the weight calculations inherent in the early design stage of a prototype (especially considering the difficulty to estimate the battery weight in a rapidly developing technology sector), it was decided that calm water predictions should be carried out for three different displacements ($\Delta 1$, $\Delta 2$ and $\Delta 3$).

3.2. Challenges in designing an electric battery-driven Fast-Ferry

For all high-speed craft, it is essential to achieve a light weight as low as possible in the ship design process. For an electric battery-driven fast vessel, a major part of the lightship weight needs to be dedicated to the battery weight.

Though the developments in the battery technologies were drastic in recent years, the energy densities of the batteries in terms of both the energy per weight and per volume are much lower than the conventional fossil fuels, such as diesel, see Fig. 6. Note that the comparable gravimetric energy density of diesel fuel (abt. 11,940 kWh/ton) is about 66 times higher than for the batteries (abt. 180 kWh/ton) [2]. Considering a typical efficiency of diesel engines of about 40%, this ratio reduces to about 26, which is still substantial. When aiming at the same weight carried by the vessel for the propulsion purpose (including engine, gear box, motor and fuel/battery etc.), the ratio of available energy for propulsion would be 10 times higher when comparing the diesel-driven vessels with the battery-driven vessels. This brings one of the challenges in designing an electric battery-driven fast-ferry, which makes the hydrodynamic optimisation indispensable to make use of the very limited energy on board as efficient as possible. More challenges in designing electric fast vessels related to operational profile, recharging of the battery, safety issues and battery life have been reviewed by one of the authors and more details can be found in [2].

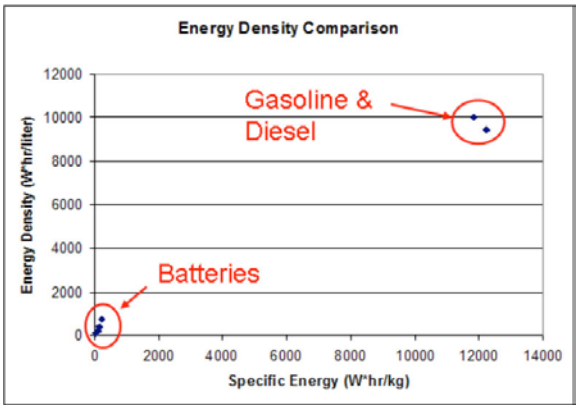

Figure 6. Energy density per weight and volume for Batteries and different fuels (source: http://energyresourcefulness.org/)

3.3. Timelines of the Development

Based on the specification of the vessel, an initial design and general arrangement has been made by the shipyard Fjellstrand and ship operator Kolumbus (both are partners in TrAM project) in May 2019, see Fig. 7. In this initial design, the battery racks have been placed into two demihulls to save space on the main deck and shift

the weight to lower parts of the hull. Based on this initial arrangement and the preliminary lines plan of a reference vessel, a parametric model for the demihulls of the Stavanger demonstrator was developed by use of the CAESES® software platform. Through the embedded optimisation algorithm within CAESES® software platform, an intensive optimisation loop has been conducted, which consists of two stages: 1. global optimisation referring to the determination of the main dimensions and integrated hull form characteristics minimising the calm water resistance; 2. Local optimisation focusing on the optimal form of the stern tunnel area and the propeller-hull-rudder interaction aiming on high propulsive efficiency. This optimisation work has been accomplished by September 2019, so that the optimal hull form has been selected for the model manufacturing. The model testing campaign took place in December 2019.

After reviewing the first model testing results and in the meantime some safety concerns were raised, it has been decided in Jan. 2020 to change the general arrangement and to move the battery racks back to the main deck (see Fig. 8), which has several advantages: 1. The limit on the width of demihull has been removed so that the optimisation can be run in larger design space and a demihull form with smaller resistance might be found; 2. The maintenance personnel has now much better access to the battery racks and it is also easier to fulfil the requirement on ventilation and safety requirement related to firefighting; 3. From the safety point of view, it is a better concept to put the battery on the main deck in case of a collision/grounding, or even a fire accident.

A new optimisation loop has been started based upon the new general arrangement and requirement. Due to the very limited timeframe and thanks to the established optimisation process, the second optimisation campaign with both global and local optimisation stages has been completed in a record tempo, which is within one month, so that the new model based on the new hull form could be manufactured in April 2020 and the second model testing campaign has taken place in May 2020.

In the following section, some details about the hydrodynamic optimisation process will be given.

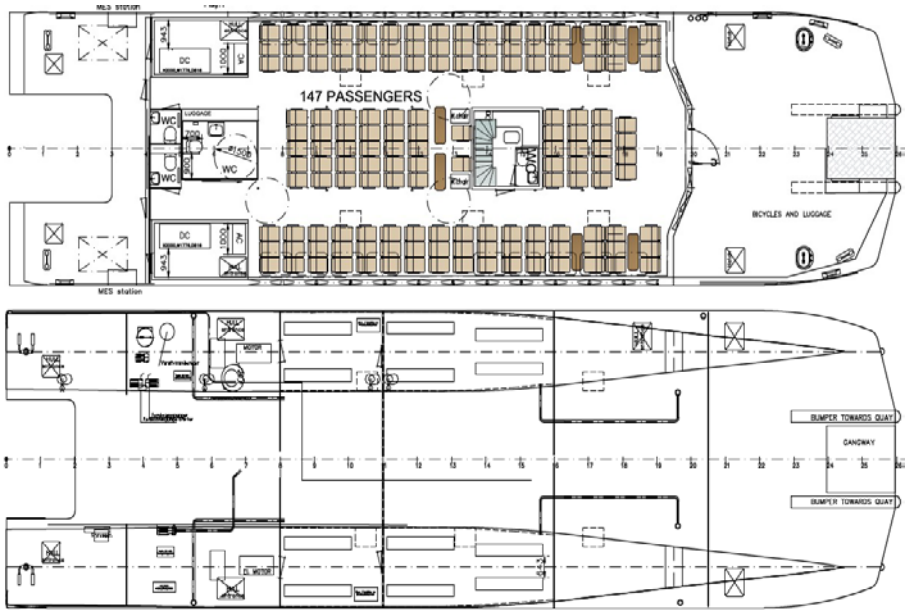

Figure 7. Initial general arrangement of the Stavanger Demonstrator

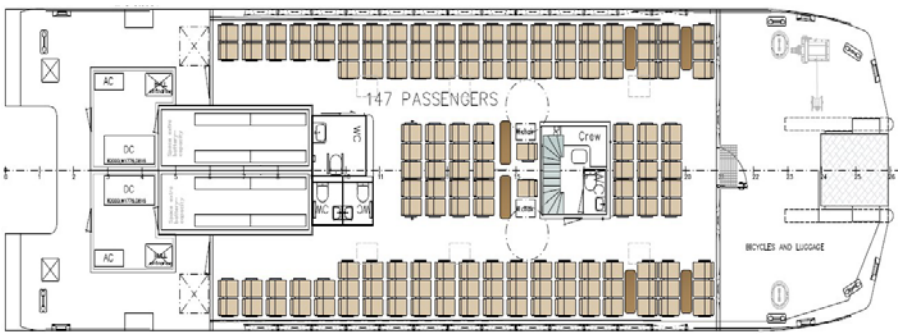

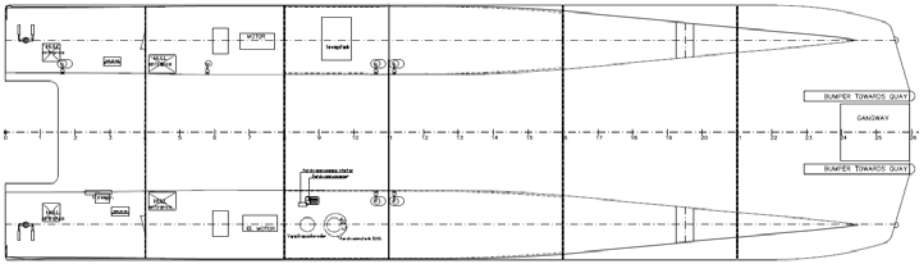

Figure 8. Final general arrangement of the Stavanger Demonstrator

3.4. Parametric Model and Optimisation Process

The developed parametric model by use of the CAESES® software platform offers the designer the possibility to control/specify the main particulars of the demihull along with the hullform details within a reasonable range of variation of the defined design variables, while at the same time adequate quality (fairness) of the hull is ensured. The designer is enabled to explore the huge design space of automatically generated hull forms and decide on the most favourable ones on the basis of rational, holistic criteria [16].

The overall beam of the catamaran has been kept constant due to design/construction reasons (yard's specification of deck superstructure module). It is of course acknowledged that increasing the separation distance of the demihulls would possibly lead to lower wave resistance at some speeds, but the increase in lightweight and production cost is expected to outweigh this resistance benefit. It is also noted that the vessel's operational Froude number will be close to 0.70, thus far beyond of the last hump of wave resistance, thus viscous resistance will be dominant at the catamaran's service speed.

A set of 20 design variables have been selected, defining the main dimensions, as well as local hull details, such as the width, immersion and shape of transom and bow area of the vessel. A view of the parametrically defined grid is presented in Figure 9a. Subsequently, a series of metasurfaces and lofted surfaces is generated, as presented in Figure 9b. After the initial hull definition, the hydrostatic values are calculated. A Lackenby transformation is then applied in order to obtain a demihull with a longitudinal centre of buoyancy close to the expected longitudinal centre of gravity. Also, the prismatic coefficient is adjusted in order to achieve a displacement close to the desired value. The Lackenby transformation parameters are considered constant during the optimisation studies. The resulting hullform is illustrated in Figure 9c.

As stated before, a philosophy of two stage optimisations has been practiced in this design and optimisation process with its work flow shown in Fig. 10. After the parametric model has been developed, a series of so-called Design of Experiments (DoE) were carried out using the HSVA's potential code v-SHALLO, to obtain the resistance of a sufficiently large number (about 200-300 for each condition) of alternative hullforms. Based on the collected pre-computed data, surrogate models were developed, enabling the sufficiently accurate estimation of the hydrodynamic quantities of interest during the optimisation study in practically zero time (in our case the calm water resistance of each design variant at various displacements and service speeds). Apart from drastically reducing the calculation time, surrogate models increased the robustness of the whole process by avoiding the need of remote computing.

The global optimisation studies were then carried out based on the surrogate models. From the set of 20 design parameters, the four most important referring to the catamaran's main dimensions and the transom width were selected as design variables during the global optimisation study. The remaining 16 design parameters were kept constant at their default values during the global optimisation. More details about the global optimisation results have been published and can be found in [14], which will not be repeated in this paper.

The local optimisation process has been started after the global optimisation with the best hull form found in the global optimisation results. The focus was put on the stern region with incorporated propeller model and the rudder geometry. The most important parameters are the transom height at centreline and the height difference from centreline to chine at transom. Negative values of the latter parameter indicate designs with chine located lower than centreline, forming the propeller tunnel area. More details about the local optimisation results could be found in [15].

After the local optimisation, a series of so-called off-deign conditions (a combination of displacements and speeds) have been evaluated with the best hull form found to make a final check and assess the overall performance of the optimised hull form.

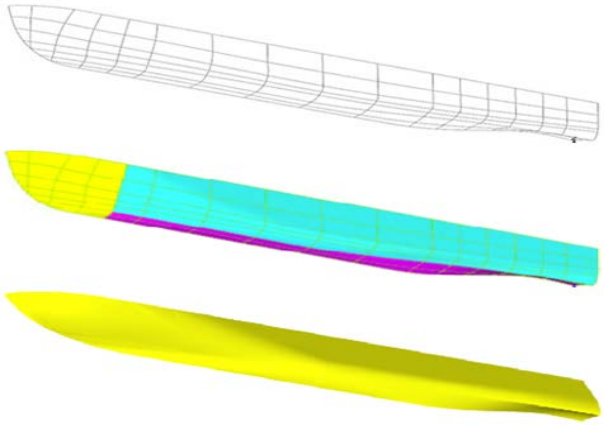

Figure 9. Definition grid (a), resulting surfaces (b) and final demihull after Lackenby transformation (c)

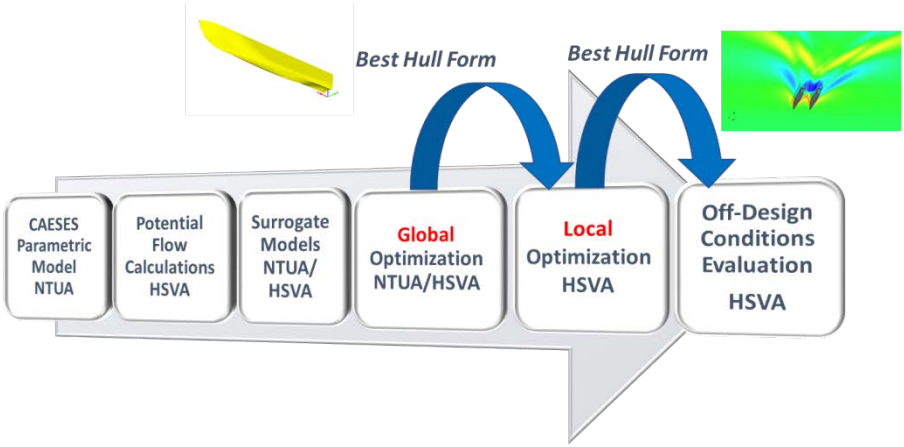

Figure 10. Work flow of optimisation process

3.5. Outline of the Optimisation Results

A large number of optimisation studies were carried out for both optimisation loops. In Fig. 11, some representative results of the global optimisation study from the first optimisation loop are illustrated. Out of 1,000 produced designs, the 824 were feasible, whereas 176 violated at least one of the constraints (marked in red). The optimum design is marked in the figures with a green circle. As can be seen, the calm water resistance shows a linear dependency on the beam of demihull at the speed of 21 kn (Fig. 11a); whereas it is not anymore the case at the speed of 25 kn due to the wave interaction of both demihulls (Fig. 11 b). Based on the defined criteria (incorporating the vessel operational profile) for global optimisation, the overall optimum design found from the first optimisation loop has a very slender hullform with a length at WL close to the maximum, a beam close to the minimum and increased draught.

As mentioned before, the minimum beam was a constraint made on the width of demihulls due to the space requirement to allocate the battery racks within the demihulls from the initial GA, which has been relaxed through the revision of the GA. Shifting the battery racks to the main deck in the final version of the GA gave more freedom for the optimisation engine being able to explore a larger design space during the second global optimisation loop.

Keeping the vessel displacement constant and the length constraint unchanged, a design with a narrower demihull beam can be found, which leads to a higher draft and also a larger wetted surface in this case. This has been expressed in the changes in the relative portion of the frictional resistance to the total resistance during the second optimisation loop comparing to the best hull form found in the first optimisation loop (marked in red), as shown in Fig. 12 (left). On the other hand, the advantage of a narrower demihull beam would be the effect of reducing the relative portion of wave resistance to the total resistance, as shown in Fig. 12 (right). The reduction

of the wave resistance has been achieved by the design of a more slender hullform with lower demihull resistance and by reducing the interaction effects by increasing the distance between the demihulls. The wave resistance reduction can also be observed when comparing the free surface deformation of the best hull forms found in the first (Fig. 13 left) and second (Fig. 13 right) optimisation loop based on the initial and final GA respectively, where the magnitudes of both wave crest and wave tough became smaller in case of the best hull form found in the second optimisation loop. In total, the removal of constraints on the demihull beam led to a new hull form that proved significantly better than the originally optimized hull form, namely by more than 6% at design speed and even more than 10% at intermediate speeds, as elaborated in later sections.

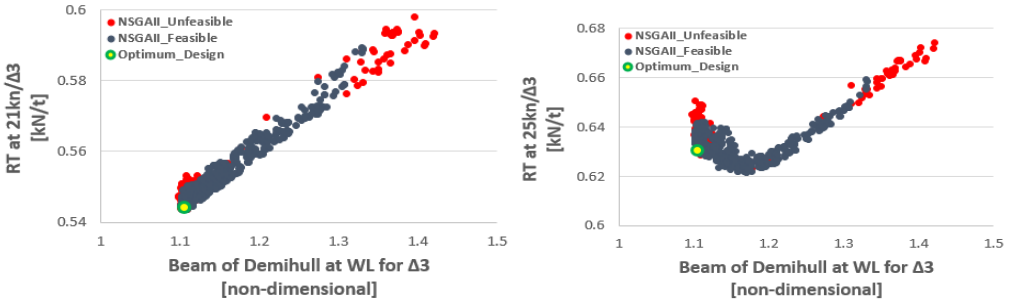

(a) 21kn (b) 25kn

Figure 11. Calm water resistance per ton of displacement against non-dimensional Beam at WL at 21kn (a) and 25 kn (b) for Δ3 from the first optimisation loop based on the initial GA

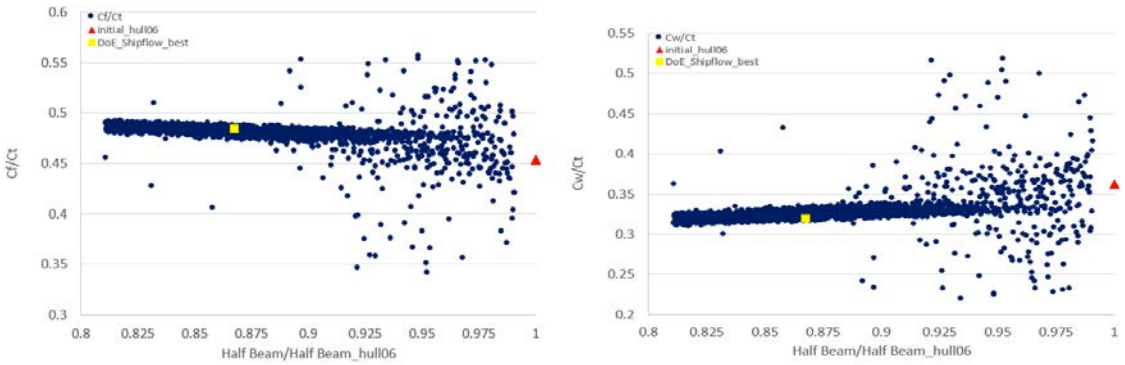

Figure 12. Relative changes in frictional resistance (left) and wave resistance (right) of the newly found best hull form (marked in yellow) against non-dimensional Beam at WL comparing to the found best hull form (marked in red) from the first optimisation loop based on the initial GA

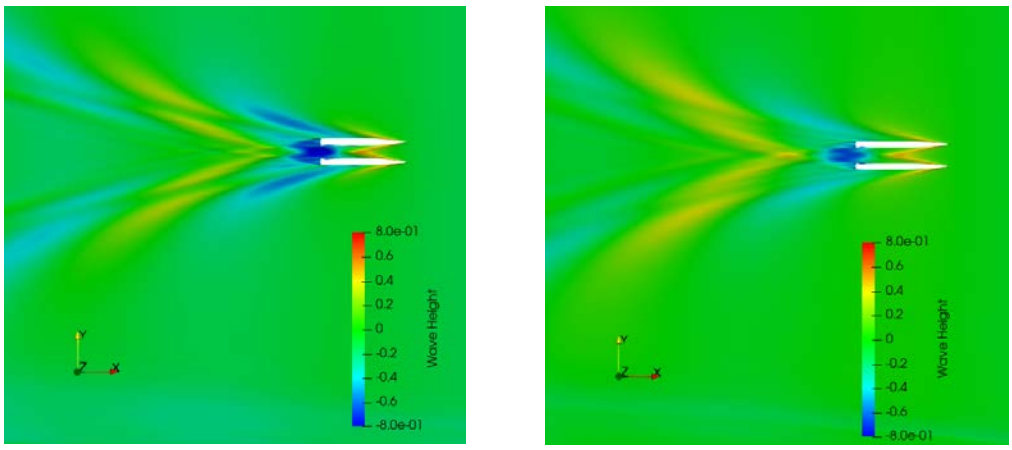

Figure 13. Free surface deformation of the best hull form found in the first (left) and second (right) optimisation loop based on the initial and final GA respectively

4. Model Tests and Validation of CFD results

As an essential part of the design process of a highly complex and innovative ship, physical model testing plays a crucial role in the verification of the anticipated full-scale speed-power performance and provides valuable data for the CFD validation purpose.

4.1. Tested Model

The determination of a suitable model scale ratio is one of the first and most important steps in the process of planning a model test campaign. The principle goal of minimizing scale effects by building a large model needs to be balanced with limiting factors such as basin constraints, carriage speed, estimated loads, measurement equipment and certainly building costs. For the TrAM model a very good trade-off between these factors resulted in a scale ratio of 1/5.6, namely a 5.34m long catamaran model. This allowed very precise measurements and minimized scale effects. The two separate demi-hull models were manufactured out of thin layer wood and were coupled by high-strength metal beams. Proper alignment and positioning of the demi-hulls was ensured by special high precise measurement gauges individually designed for this test setup. A view of the stern area of the model with fitted CP propellers and (twisted) rudders is shown in Figure 14.

Figure 14. View of the stern area of the tested Stavanger model, with fitted propellers, shafts, brackets and rudders

4.2. Test Scope

The calm water model tests were carried out in HSVA's large basin which is 300 m long, 18 m wide and 6 m deep. The speed of the model ranged from 1.5 to 6.5 m/s, which corresponds to a ship speed of 8 to 29 knots. During the test runs all relevant forces and movements of the model have been recorded, while also including wave profile measurements for the generated wave wash downstream. The test program included both towing resistance and self-propulsion tests for three different displacements $\Delta 1$, $\Delta 2$, $\Delta 3$ and a range of trims. A systematic variation of the static pre-trim of the vessel delivered valuable information for a beneficial arrangement of the ship's weight distribution in terms of power reduction. The entire test series was live-broadcasted ("live-stream") and recorded by several cameras showing the model and the flow around it from different perspectives, as shown in Fig. 15. This allowed a detailed observation of the vessel's hydrodynamic behaviour remotely and even after the tests, as necessary. As stated before, a 1st test campaign with the originally optimised hull form (battery racks placed in the demihulls) was conducted in December 2019 followed by a 2nd campaign repeated the test series for the finally selected hull form in May 2020.

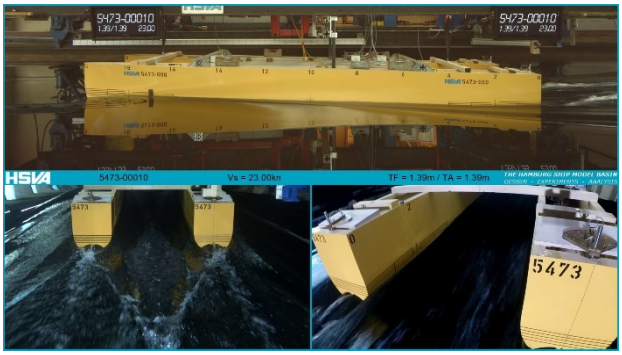

Figure 15. Self-propulsion model of the Stavanger demonstrator at at 23 knots full scale speed

4.3. Outline of Test Results

In the conducted second test series with the revised hull form (May 2020) the resistance and propulsion power could even be reduced significantly for the relevant speed range above 14 knots. The calm water resistance and power requirement has been reduced by abt. 6.1% at design speed of 23 knots and over 10% at the speed range of 15-17 knots (see Fig. 16).

Besides the variation of the calm water resistance for tested conditions, special attention was paid to the propulsive efficiency of the fitted propulsion plant and the hull-propeller-rudder interaction (wake and thrust deduction factors) (a detailed analysis on these results can be found in [15]). A remarkable result of the model tests was the extraordinarily high propulsive efficiency that could be achieved thanks to the refined local optimisation of the hull-propeller interaction. Figure 17 compares the measured propulsive efficiency of the TrAM Demonstrator in comparison with other propulsion systems in the literature. The very low thrust deduction fraction on the one hand and the achievement of a hardly disturbed propeller inflow condition on the other side resulted in a propulsion efficiency of 77% at design speed and up to 80% at higher speeds.

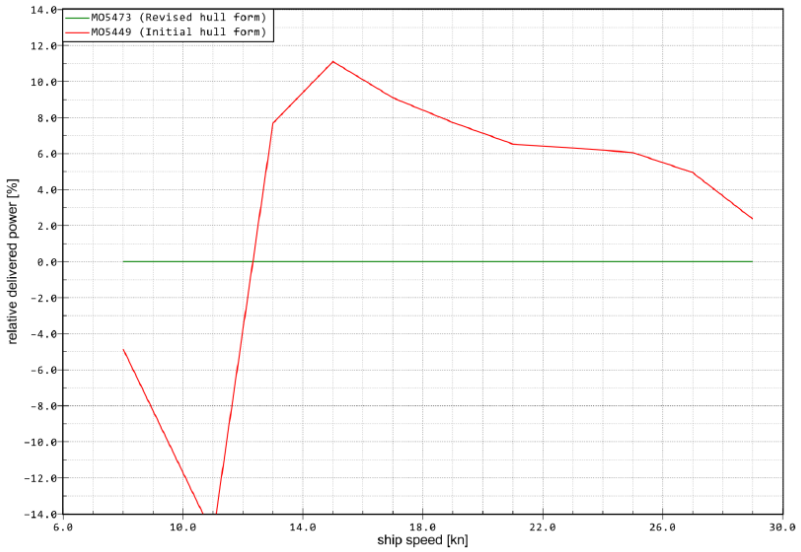

Figure 16. Model tests prediction of rated delivered power: revised hull form vs. initial hull form

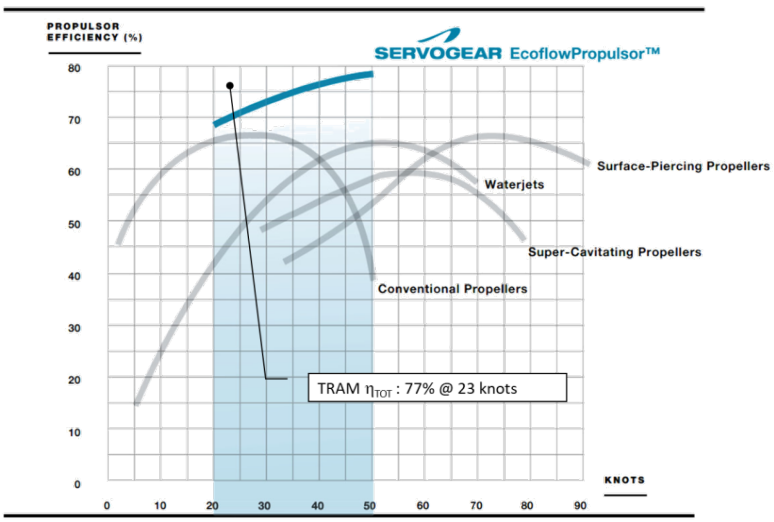

Figure 17. Propulsion efficiency achieved by the TrAM Demonstrator compared to other propulsion systems (source: www.servogear.no)

4.4. Validation of CFD Results

The numerically predicted model and full-scale values obtained by CFD simulations could be very well confirmed by the test campaigns. Figure 18 shows the comparison on the rated resistance (left) and delivered horsepower under trail condition (right) for the Stavanger Demonstrator between model experiments and CFD calculations by HSVA using the RANS code FreSCO+. The deviation between experiments and CFD is abt. 3% in average. As mentioned before, the wave profile measurements have also been conducted using four wave probes, whose positions are given in Fig. 19. Figure 20 shows the comparison of the measured wave height with CFD predictions (without and with the propeller action) at the corresponding four wave probes with the marked AP and FP representing the forward and after perpendiculars of the vessel respectively. Again good agreement on the primary wave height can be observed. It should be noted that the grids applied for this study have been refined only in the region of one Lpp beside and behind the vessel, therefore they are not really fine beyond that region and some numerical damping can be observed in the far field accordingly.

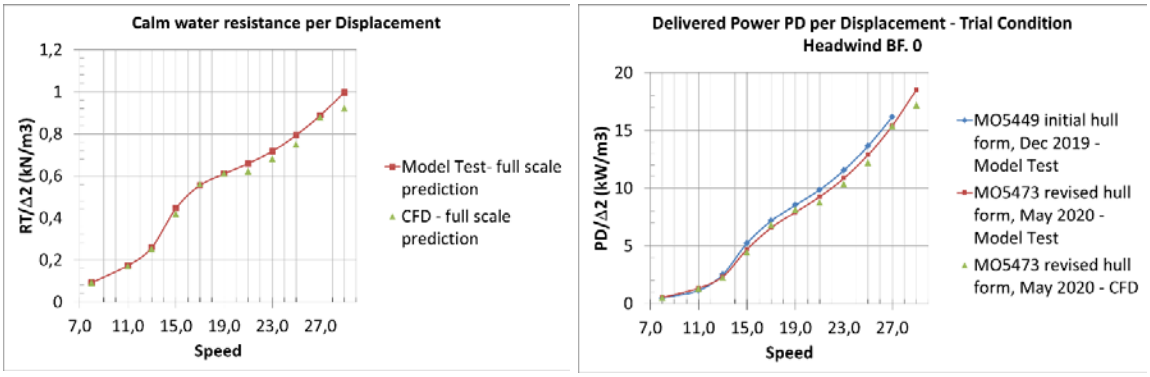

Figure 18. Prediction of the rated full-scale calm water resistance (left) and delivered horsepower under trail condition (right) for the Stavanger Demonstrator on the basis of model experiments and CFD calculations by HSVA (initial and revised hull form)

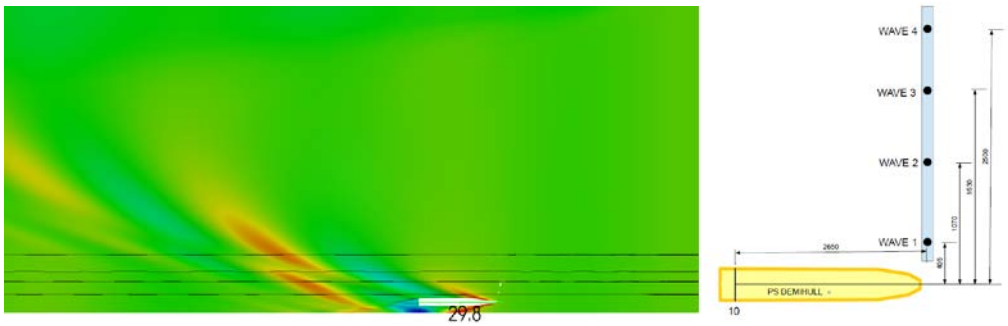

Figure 19. Positions (in model scale) of the wave probes beside the vessel

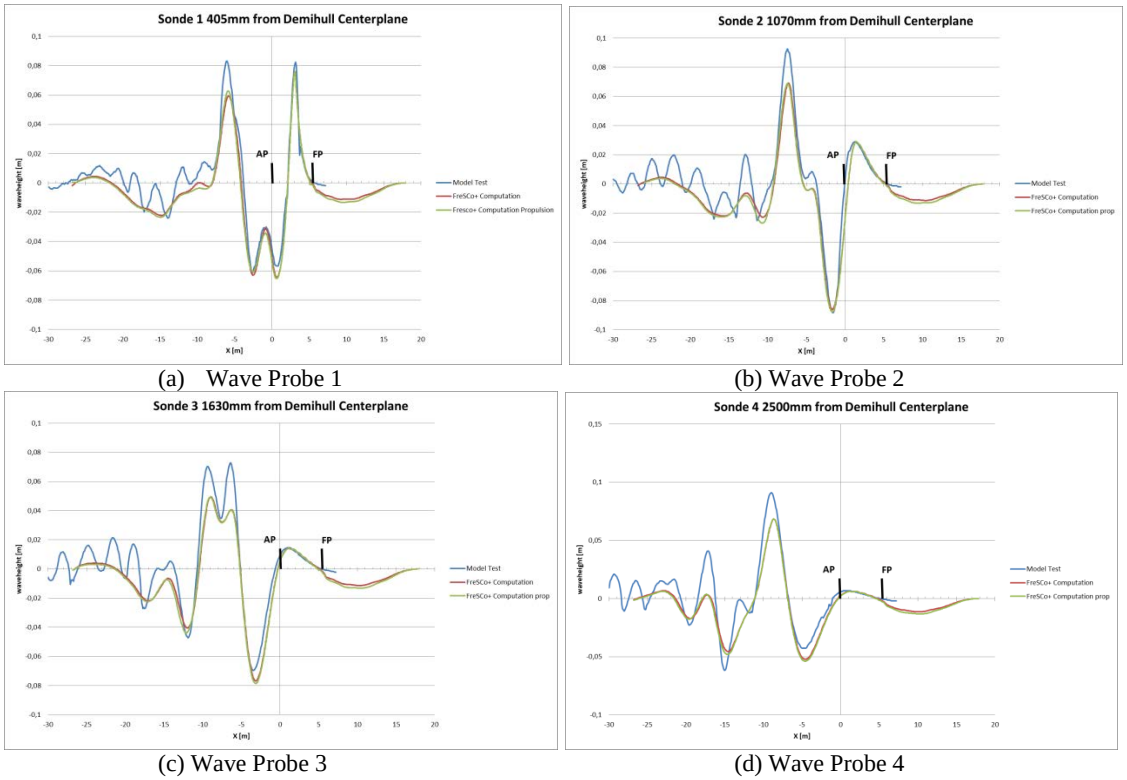

(a) Wave Probe 1 (b) Wave Probe 2

(c) Wave Probe 3 (d) Wave Probe 4

Figure 20. Comparison of the measured wave height with CFD predictions (without and with propeller action) at the four (4) wave probes with the marked AP and FP representing the forward and after perpendiculars of the vessel respectively

5. Seakeeping Predictions

After the hull form and propulsion unit optimisation was completed, a detailed structural design of the vessel was accomplished by the shipyard Fjellstrand. In the meantime, further investigations on the seakeeping behaviour have been conducted by the partners NTUA and HSVA to access the seakeeping response of the Stavanger Demonstrator. The aim of this study is to deliver the assessment of the criteria specified by IMO rules [17], where limiting values for the maximum acceleration are set to describe the level of safety degradation.

Calculations were carried out using NTUA in-house 3D panel code NEWDRIFT to obtain the motions responses in 6 degrees of freedom (DOF), assuming regular, sinusoidal waves of different wavelengths and directions. Furthermore, three vessel speeds and two loading conditions were considered. The motion responses calculated by the panel code NEWDRIFT have been checked at some conditions against the results from the RANS code FreSCO+ by HSVA, since it is well known that the potential code often over-estimates the ship responses in the resonance region while neglecting the viscous damping and non-linear effects.

Final goal of this study is the prediction of the expected maximum accelerations at several points of interest on the hull, assuming realistic seaways, characterized by sea spectra of specific parameters. To proceed with this

type of calculation, standard spectral analysis method is employed, under the assumption of linearity of responses. This process leads to the response spectrum at every point of interest, from which the RMS and maximum accelerations can be evaluated.

5.1. Case description

For the discretization of the hull, a total number of 1330 panels were used for each demi-hull by NEWDRIFT, 820 of which are used to represent the wetted surface and another 510 panels represent the deck lid (for removing the irregular frequencies, see [7]). Furthermore, three different speeds were considered, namely zero speed of advance, 19kn and 23kn. The calculations are performed for head seas (180deg) and beam seas (90deg). Following meteorological statistics in the area of operation, the wavelengths selected cover a range from 0.6m up to 79m, corresponding to a range from 0.02Lpp to 2.65Lpp, where Lpp is the ship length between perpendiculars.

The chosen Pierson-Moskowitz sea-spectrum for the case study (in accordance to the specification of the authorities) is characterized by the combinations of peak period and significant wave height, as shown in Table 1.

Table 1. Pierson-Moskowitz parameters

Hs [m]	Tp [sec]
0.50	2.20
1.00	3.80
1.50	4.90

For each sea state the vertical and horizontal accelerations RMS values for a series of points of interest need to be evaluated. The coordinates of these points are listed in the Table 2 and they were defined based on a General Arrangement Plan of the catamaran, as presented in Figure 21.

Figure 21. Points of interest marked on the General Arrangement plan

Table 2. Coordinates of points of interest

Point of Interest ID	x [m] (from AP)	y [m] (from centerplane)	z [m] (from baseline)
#1	24.3	0.0	4.0
#2	24.7	3.8	4.0
#3	24.7	-3.8	4.0
#4	15.1	0.0	4.0
#5	10.4	3.8	4.0
#6	7.9	-3.8	4.0
#7	5.5	-4.5	4.0

For each point of interest, the maximum accelerations, considering the selected sea spectra are evaluated and checked against the specified criteria. It should be noted at this point that the ability of the propulsion plant of the vessel to maintain a forward speed of 19 kn or 23 kn in the specified sea conditions and to overcome the increased power demand due to the added resistance in waves was not considered in the current study.

5.2. Seakeeping Results

The seakeeping results obtained for the vessel by both the potential theory panel code NEWDRIFT and the RANS CFD code FreSCO+ are presented in this section. The Response Amplitude Operators (RAOs) curves for the centre of gravity (CG) have been compared with results obtained from both methods for the different headings and vessel speeds. Calculated RMS values for motions, velocities and accelerations at the onboard points of interest were obtained by NEWDRIFT and parts of it ate presented in Table 3.

RAOs are given in non-dimensional form, with the linear motion amplitudes normalised by the wave amplitude $\hat{\zeta}$ and the rotations by the wave steepness, as shown below:

$$\mathrm{RAO}_z = \frac{z}{\hat{\zeta}} \tag{1}$$

$$\mathrm{RAO}_\theta = \frac{\theta}{k\zeta}, \quad \text{where} \quad k = \frac{2\pi}{\lambda} \tag{2}$$

The nondimensional added resistance coefficients are defined by:

$$C_{AW} = \frac{R_{AW}}{\rho g (B^2/L_{WL}) \cdot \hat{\zeta}^2}\ , \tag{3}$$

where R_{AW} represents the difference between resistance in waves and calm water resistance, B is the beam of the demihull and L_{WL} is the ship's length at waterline.

Figure 22 shows the comparison of predicted heave (left) and pitch (right) RAO curves by the panel code NEWDRIFT and the RANS code FreSCO+ in head seas at three different ship speeds. As could be expected, the potential theory panel code NEWDRIFT over-predicts the RAOs in the heave-pitch resonance region, compared to the RANS code, while at zero ship speed both calculated RAOs have comparable values and converge to "1" for long waves, as could be expected. It is confirmed that a linear potential theory method without consideration of nonlinear effects that dominate regions of heave/pitch resonance (that will lead to the emergence of the shallow draft catamaran's ends, green water on deck and to increase of motion damping, as indicated in Figure 23 by four snapshots of free surface deformation and wave system of TrAM catamaran at ship speed V = 19kn in head sea (H = 1.5m and T = 4.9s) within one wave period) will always predict larger motions and accelerations and therefore it is more conservative in terms of fulfilling the IMO criteria. Note that based on meteorological statistics, the probability that the study vessel encounters waves of period larger than abt. 3 seconds and wave heights larger than abt. 0.6m in the Stavanger area of operation is year-round practically zero [18].

The CAW computed by the RANS code FreSCO+ is shown in Fig. 24, which can be used to estimate additional required power of the vessel in waves at certain speed.

Similar trends can be observed when comparing the RAOs of roll motion predicted by the panel code NEWDRIFT and the RANS code FreSCO+ in beam seas at different speeds (see Fig. 25). The panel code again over-predicts the RAO values, but the peaks are predicted at almost the same frequencies. It is important to briefly comment on the complicated roll motion of a catamaran, compared to a monohull. The roll motion of the catamaran essentially differs from that of a monohull in view of the motion of the two demihulls: the demihulls are practically undergoing heave-pitch motions in the transverse reference plane and may emerge from water in case of resonance, what is a highly nonlinear phenomenon. Even more, additionally internal flow resonances in the region between the two demihulls seem to occur with the incoming wave running beam wise as indicated by Fig. 26, showing two snapshots of free surface deformation and wave system at ship speed V = 19kn in beam sea of T = 3.4s.

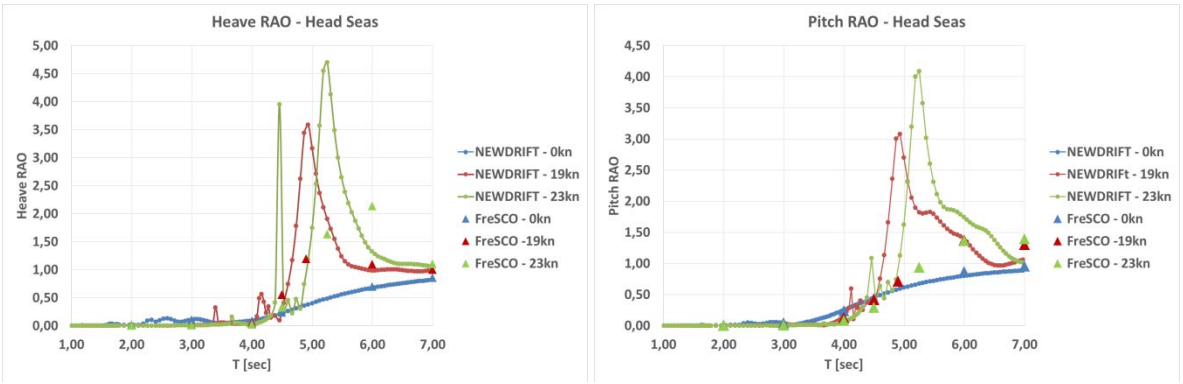

Figure 22. Comparison on predicted heave (left) and pitch (right) RAOs by the panel code NEWDRIFT and the RANS code FreSCO+ in head seas at different ship speeds

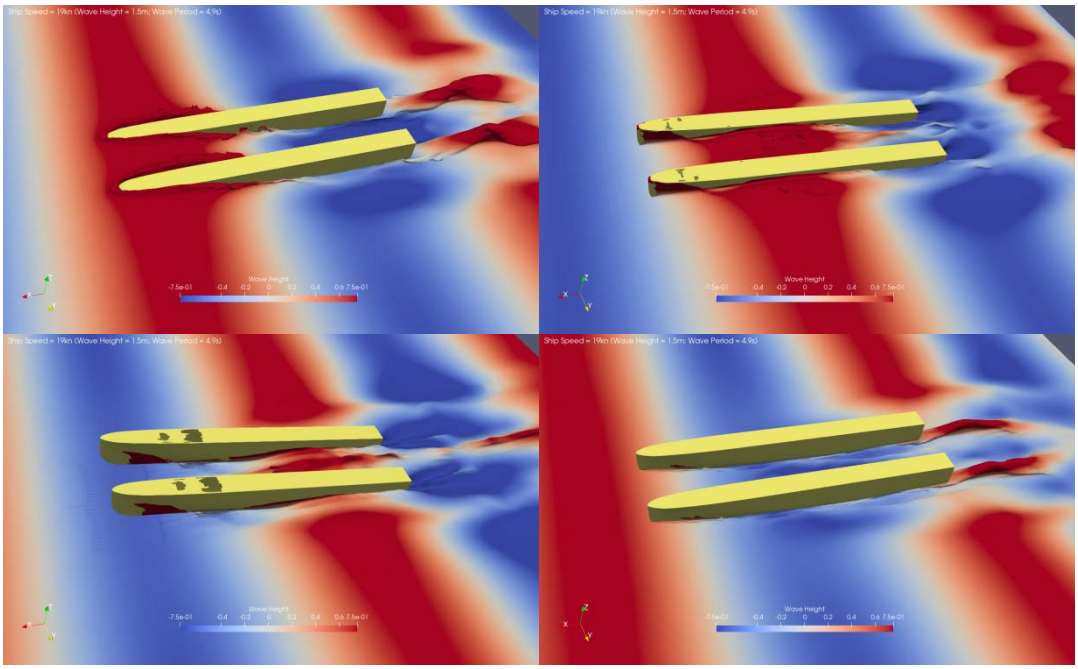

Figure 23. Four Snapshots of free surface deformation and wave system of TrAM catamaran at ship speed V = 19kn in head sea (H = 1.5m and T = 4.9s) within one wave period

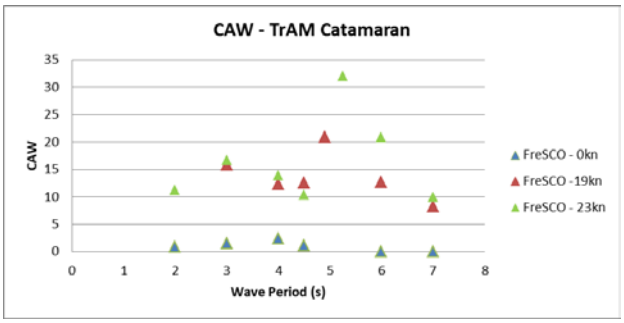

Figure 24. Computed CAW by the RANS code FreSCO+ in head seas at different ship speeds

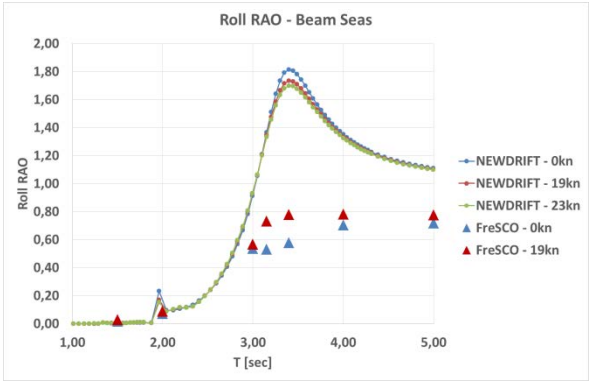

Figure 25. Comparison on predicted Roll RAOs by the panel code NEWDRIFT and the RANS code FreSCO+ in beam seas at different ship speeds

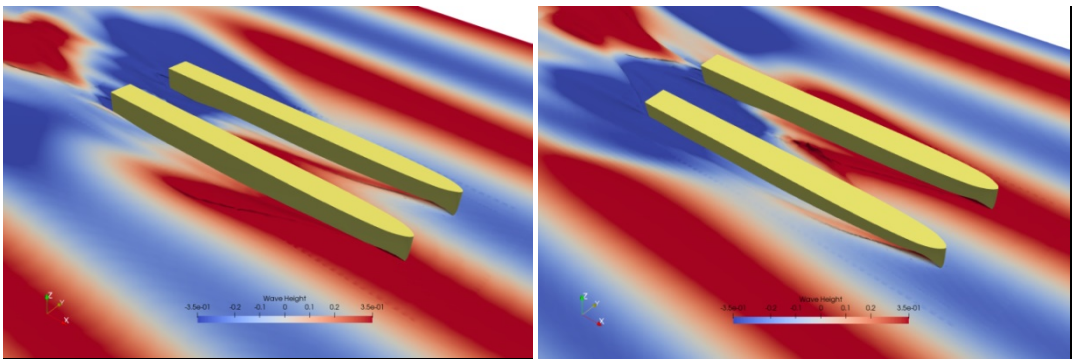

Figure 26. Snapshots of free surface deformation and wave system of TrAM catamaran at ship speed V = 19kn in beam sea of T = 3.4s

For the irregular seas' response, the criteria defined in [17] for level 1 and level 2, regarding the maximum horizontal accelerations are checked for each spectrum and ship speed. A summary of the results regarding the criteria are given in Table 3 for head seas. For beam seas, it appears that some criteria are not fulfilled for spectral seaways with Hs=1.0m/Tp=3.8sec and Hs=1.5m/Tp=4.9sec, namely level 1 criteria are not satisfied, implying a moderate degradation of safety and some level of discomfort, according to the Code, while at the same time, the strict safety level 2 criteria are always and everywhere fulfilled. It must be noted, that the herein presented accelerations are based on a potential theory code without viscous damping motion corrections, what is essential especially for the predicted peaks of roll motion, thus an over-prediction of the responses is anticipated. Furthermore, the spectral characteristics of the seaways considered, represent an envelope of life-cycle worst-case scenarios anticipated for the study ship, in order to be on the safe side during the design phase, neglecting also possible operational measures to avoid excessive motions and accelerations, such as speed and course change to avoid beam seas and weather routeing to avoid heavy seas. Last but not least, the probability that the study ship encounters waves of period larger than about 3 sec in the Stavanger area is practically zero based on meteorological statistics [18].

Table 3. Maximum horizontal accelerations for head seas & criteria assessment

Point	Spectrum	Hs=0.5	Tp=2.2	
	Vs	0kn	HEAD SEAS	
	coord	acc (g)	Lvl 1 (0.2g)	Lvl 2 (0.35g)
1	(24.3,0,4)	0.003	✓	✓
2	(24.7,3.8,4)	0.003	✓	✓
3	(24.7,-3.8,4)	0.003	✓	✓
4	(15.1,0,4)	0.003	✓	✓
5	(10.4,3.8,4)	0.003	✓	✓
6	(7.9,-3.8,4)	0.003	✓	✓
7	(5.5,-4.5,4)	0.003	✓	✓

Point	Spectrum	Hs=0.5	Tp=2.2	
	Vs	19kn	HEAD SEAS	
	coord	acc (g)	Lvl 1 (0.2g)	Lvl 2 (0.35g)
1	(24.3,0,4)	0.010	✓	✓
2	(24.7,3.8,4)	0.010	✓	✓
3	(24.7,-3.8,4)	0.010	✓	✓
4	(15.1,0,4)	0.010	✓	✓
5	(10.4,3.8,4)	0.010	✓	✓
6	(7.9,-3.8,4)	0.010	✓	✓
7	(5.5,-4.5,4)	0.010	✓	✓

Point	Spectrum	Hs=0.5	Tp=2.2	
	Vs	23kn	HEAD SEAS	
	coord	acc (g)	Lvl 1 (0.2g)	Lvl 2 (0.35g)
1	(24.3,0,4)	0.012	✓	✓
2	(24.7,3.8,4)	0.012	✓	✓
3	(24.7,-3.8,4)	0.012	✓	✓
4	(15.1,0,4)	0.012	✓	✓
5	(10.4,3.8,4)	0.012	✓	✓
6	(7.9,-3.8,4)	0.012	✓	✓
7	(5.5,-4.5,4)	0.012	✓	✓

Point	Spectrum	Hs=1.0	Tp=3.8	
	Vs	0kn	HEAD SEAS	
	coord	acc (g)	Lvl 1 (0.2g)	Lvl 2 (0.35g)
1	(24.3,0,4)	0.018	✓	✓
2	(24.7,3.8,4)	0.018	✓	✓
3	(24.7,-3.8,4)	0.018	✓	✓
4	(15.1,0,4)	0.018	✓	✓
5	(10.4,3.8,4)	0.018	✓	✓
6	(7.9,-3.8,4)	0.018	✓	✓
7	(5.5,-4.5,4)	0.018	✓	✓

Point	Spectrum	Hs=1.0	Tp=3.8	
	Vs	19kn	HEAD SEAS	
	coord	acc (g)	Lvl 1 (0.2g)	Lvl 2 (0.35g)
1	(24.3,0,4)	0.036	✓	✓
2	(24.7,3.8,4)	0.036	✓	✓
3	(24.7,-3.8,4)	0.036	✓	✓
4	(15.1,0,4)	0.036	✓	✓
5	(10.4,3.8,4)	0.036	✓	✓
6	(7.9,-3.8,4)	0.036	✓	✓
7	(5.5,-4.5,4)	0.036	✓	✓

Point	Spectrum	Hs=1.0	Tp=3.8	
	Vs	23kn	HEAD SEAS	
	coord	acc (g)	Lvl 1 (0.2g)	Lvl 2 (0.35g)
1	(24.3,0,4)	0.043	✓	✓
2	(24.7,3.8,4)	0.043	✓	✓
3	(24.7,-3.8,4)	0.043	✓	✓
4	(15.1,0,4)	0.043	✓	✓
5	(10.4,3.8,4)	0.043	✓	✓
6	(7.9,-3.8,4)	0.043	✓	✓
7	(5.5,-4.5,4)	0.043	✓	✓

Point	Spectrum	Hs=1.5	Tp=4.9	
	Vs	0kn	HEAD SEAS	
	coord	acc (g)	Lvl 1 (0.2g)	Lvl 2 (0.35g)
1	(24.3,0,4)	0.052	✓	✓
2	(24.7,3.8,4)	0.052	✓	✓
3	(24.7,-3.8,4)	0.052	✓	✓
4	(15.1,0,4)	0.052	✓	✓
5	(10.4,3.8,4)	0.052	✓	✓
6	(7.9,-3.8,4)	0.052	✓	✓
7	(5.5,-4.5,4)	0.052	✓	✓

Point	Spectrum	Hs=1.5	Tp=4.9	
	Vs	19kn	HEAD SEAS	
	coord	acc (g)	Lvl 1 (0.2g)	Lvl 2 (0.35g)
1	(24.3,0,4)	0.069	✓	✓
2	(24.7,3.8,4)	0.069	✓	✓
3	(24.7,-3.8,4)	0.069	✓	✓
4	(15.1,0,4)	0.069	✓	✓
5	(10.4,3.8,4)	0.069	✓	✓
6	(7.9,-3.8,4)	0.069	✓	✓
7	(5.5,-4.5,4)	0.069	✓	✓

Point	Spectrum	Hs=1.5	Tp=4.9	
	Vs	23kn	HEAD SEAS	
	coord	acc (g)	Lvl 1 (0.2g)	Lvl 2 (0.35g)
1	(24.3,0,4)	0.090	✓	✓
2	(24.7,3.8,4)	0.090	✓	✓
3	(24.7,-3.8,4)	0.090	✓	✓
4	(15.1,0,4)	0.090	✓	✓
5	(10.4,3.8,4)	0.090	✓	✓
6	(7.9,-3.8,4)	0.090	✓	✓
7	(5.5,-4.5,4)	0.090	✓	✓

6. Preliminary Turning Manoeuvring Analysis

Some preliminary turning manoeuvring simulation results shall be presented here and the work is still an on-going subject in the project. Some manoeuvring sea trials are planned and will be conducted in near future.

The aim of this study is to find out the turning behaviour of the catamaran at different operational modes. The Catamaran is equipped with two bow thrusters (one in each demihull) and two controllable pitch propellers. The ship operator/owner wants to know how fast the catamaran can be turned by 180°/360° at different speeds and different settings of bow thrusters/propellers. The difficulties in such simulations are that on the one hand the simulation is highly nonlinear and complex and needs to be performed in time domain, which is very time-consuming and sometimes leads to divergence of the simulation; on the other hand the operational settings of both bow thrusters and propellers for such manoeuvring were not yet clear at the time of simulation so that some estimations/assumptions need to be made. Body force models have been employed to simulate the bow thruster and propeller actions in this study.

Basically the simulations can be divided into two modes: 1. Bow Thruster (BT) only mode: only the bow thrusters are turned on, there is no action of propellers; 2. COMBI mode: two bow thrusters and two propellers are turned on, as illustrated in Fig. 27.

Different transient simulations have been performed for different modes and settings for the “turning on the spot” scenario. As expected, one can observe an almost linear increase of the turning rate with the increased RPMs/Power of the Bow Thrusters at the “BT only” mode, as shown in Fig. 28. With the propellers turned on in addition, the turning rate of the vessel has been increased by 2 or 2.5 times in this case. The complex flow phenomena and free surface deformation can be seen in Fig. 29 and Fig. 30 at two time frames at different turning angles respectively. Figure 31 shows the corresponding propeller body forces, where the red and blue colours indicate a positive and negative propeller thrust respectively.

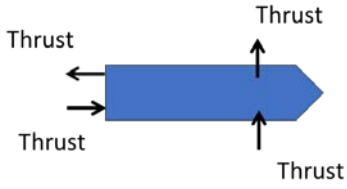

Figure 27. Illustration of the bow thrusters and propellers’ action during the “turning on the spot” manoeuvres

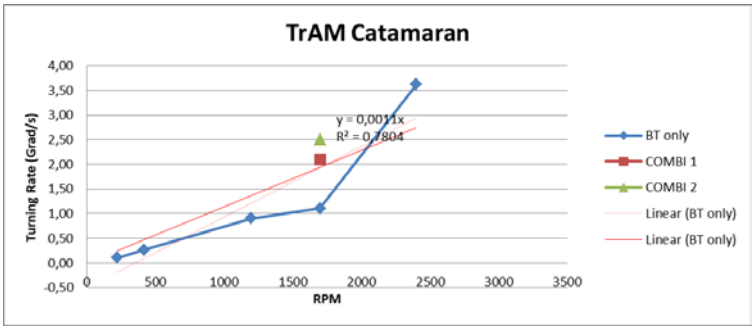

Figure 28. Computed initial turning rates by different settings of bow thrusters and propellers

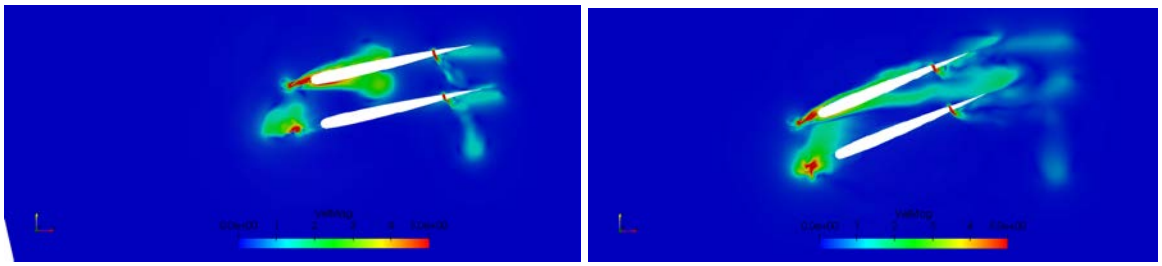

(a) t = 6.0s (b) t = 12.0s

Figure 29. Velocity magnitude on a horizontal plane showing the flow propelled by bow thrusters and propellers of TrAM catamaran during turning manoeuvres at two different turning angles

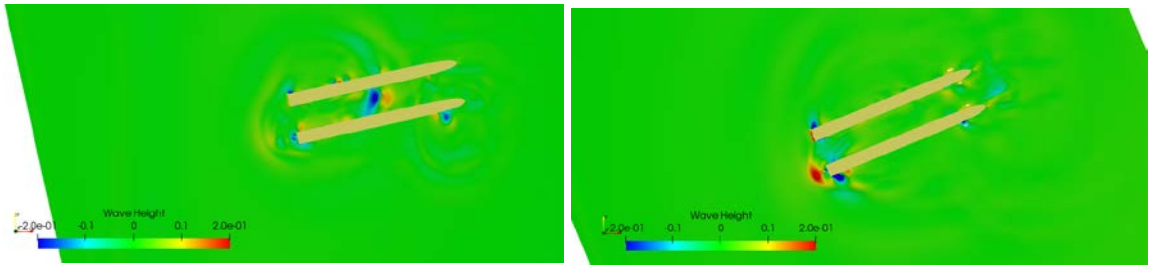

(a) t = 6.0s (b) t = 12.0s

Figure 30. Free surface deformation of TrAM catamaran during turning manoeuvres at two different turning angles

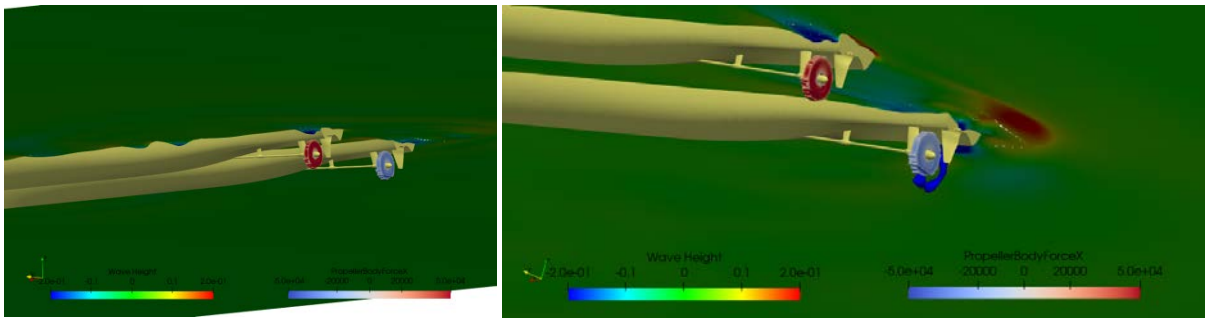

(a) t = 6.0s (b) t = 12.0s

Figure 31. Free surface and propeller body force actions of TrAM catamaran during turning manoeuvres at two different turning angles

7. Conclusions

Comprehensive numerical and experimental studies were performed in the course of development of the world first zero emission, battery driven fast catamaran Medstraum. Due to the very low energy density of

battery compared to fossil energy and thus very limited energy capacity on board, efficient use of energy became more than ever important for electric battery-driven vessels, which makes the hydrodynamic optimisation almost indispensable in the design process. The studies included the catamaran's speed-power performance in calm water, its seakeeping and manoeuvrability. The conducted optimisation led to an impressive propulsive efficiency of close to 80%, what enabled the feasibility of fast, battery-driven waterborne vehicle. The seakeeping performance of the vessel in the area of operation around Stavanger is satisfactory and in compliance with the provisions of High-Speed Code (HSC2000) for the Level 2 Major Effect criteria. The same applies to the manoeuvrability of the vessel that is equipped with four propulsor units (two CP propellers and 2 bow thrusters), turning in limited waters as expected by the operator. Delivery trials of the vessel are due in June 2022 and will be reported in future publications.

Acknowledgments

The authors are thankful to Johannes Strobel and Scott Gatchell (HSVA), Andreas Prinz (Servogear), Edmund Tolo and Morten Berhovde (Fjellstrand Shipyard) and Mikal Dahle (Kolumbus), for their contributions to the presented work. The TrAM project has received funding from the European Union's Horizon 2020 research and innovation programme under grant agreement No 769303.

References

[1] TrAM - Transport: Advanced and Modular, *H2020 EU research project*, Grant Agreement No 769303, H2020, https://tramproject.eu/, 2018-2022.

[2] Papanikolaou, A., Review of the Design and Technology Challenges of Zero-Emission, Battery-Driven Fast Marine Vehicles, *Journal of Marine Science and Engineering, MDPI*, 2020, 8, 941.

[3] Jensen, G. H.; Mi. Z. Söding X. Rankine source methods for numerical solutions of the steady wave resistance problem. *In Proc. 16th Symposium on Naval Hydrodynamics*, Berkeley, 1986.

[4] Gatchell, S.; Hafermann, D.; Jensen, G.; Marzi, J.; Vogt, M.; Wave resistance computations - A comparison of different approaches. *In 23rd Symp. Naval Hydrodynamics* (ONR), Val de Reuil, 2000.

[5] Papanikolaou, A. 1985. On integral-equation-methods for the evaluation of motions and loads of arbitrary bodies in waves. *Ingenieur-Archiv* 55: 17-29.

[6] Papanikolaou, A., Schellin, Th., "A Three-Dimensional Panel Method for Motions and Loads of Ships with Forward Speed", Journal Schiffstechnik - Ship Technology Research, Vol. 39, No. 4, pp.147-156,1992

[7] Dafermos, G. K., Zaraphonitis, G. N., & Papanikolaou, A. D. (2019, August). On an extended boundary method for the removal of irregular frequencies in 3D pulsating source panel methods. In Sustainable Development and Innovations in Marine Technologies: *Proceedings of the 18th International Congress of the Maritme Association of the Mediterranean (IMAM 2019)*, September 9-11, 2019, Varna, Bulgaria (p. 53). CRC Press.

[8] Hafermann, D.; The New RANSE Code FreSCo for Ship Application, *Jahrbuch der Schiffbautechnischen Gesellschaft*, Vol. 101, 2007

[9] Ferziger, J. H. ; Peric, M. Computational Methods for Fluid Dynamics. *Springer Verlag*, 3rd edition, 2002.

[10] Jensen, G., Klemt, M., Xing-Kaeding, Y. On the way to the Numerical Basin for Seakeeping anf Manoeuvring, *Proceeding of the PRADS'04*, 2004

[11] Chao, K. Y. ; Streckwall, H. Berechnung der Propellerumströmung mit einer Vortex-Lattice Method. *Jahrbuch der Schiffbautechnischen Gesellschaft*, Band 83, 1989.

[12] Xing-Kaeding, Y.; Gatchell, S. ; Streckwall, H. Towards Practical Design Optimisation of Pre-Swirl Device and its Life Cycle Assessment. *Fourth International Symposium on Marine Propulsors, SMP'15*, Austin, Texas, USA, June 2015.

[13] Kanellopoulou, A.; Xing-Kaeding, Y.; Papanikolaou, A.; Zaraphonitis, G. Parametric Design and Hydrodynamic Optimisation of a battery-driven fast catamaran vessel. *In Proc. RINA Conf. on Sustainable and Safe Passenger Ships*, 4th March 2020, Athens, Greece.

[14] Papanikolaou, A., Xing-Kaeding, Y., Strobel, H., Kanellopoulou, A., Zaraphonitis, G., Tolo, E., Numerical and Experimental Optimisation Study on a Fast, Zero Emission Catamaran, *Journal of Marine Science and Engineering, MDPI*, 2020, 8, 657.

[15] Xing-Kaeding, Y. and Papanikolaou, A., Optimisation of the Propulsive Efficiency of a Fast Catamaran, *Journal of Marine Science and Engineering, MDPI*, 2021, 9, 492.

[16] Papanikolaou A.; Holistic Ship Design Optimisation. *Journal Computer-Aided Design*. Vol. 42, Issue 11, pp. 1028-1044, Elsevier, pp. 1028-1044, 2010.

[17] HSC 2000 Code - International Code of Safety for High-Speed Craft, 2000 – Resolution MSC.97(73), Chapter 17, *https://imorules.com/HSC2000_CH17.html*

[18] Aarnes, J. O., METreport - Bølgeforhold ved Vassøy – Stavanger, *Norwegian Meteorological Institute*, ISSN 2387-4201, Nov. 2020.